Published in final edited form as:
*J Immunol*. 2013 July 15; 191(2): 572–582. doi:10.4049/jimmunol.1300299.

# The mechanism of splenic iNKT cell activation dictates localization in vivo

**Irah L. King**[*,†], **Eyal Amiel**[*], **Mike Tighe**[*], **Katja Mohrs**[*], **Natacha Veerapen**[‡], **Gurdyal Besra**[‡], **Markus Mohrs**[*,§], and **Elizabeth A. Leadbetter**[*,§,¶]

[*]Trudeau Institute, Saranac Lake, NY, USA

[‡]University of Birmingham, Birmingham, UK

## Abstract

Invariant Natural Killer T (iNKT) cells are glycolipid-specific innate lymphocytes emerging as critical players in the immune response to diverse infections and disease. iNKT cells are activated either through cognate interactions with lipid-loaded antigen-presenting cells, by antigen-independent cytokine-mediated signaling pathways, or a combination of both. While each of these modes of iNKT cell activation play important roles in directing the humoral and cell-mediated immune response, the spatio-temporal nature of these interactions and the cellular requirements for activation are largely undefined. Combining novel in situ confocal imaging of αGalactosylceramide-loaded CD1d tetramer labeling to localize the endogenous iNKT cell population with cytokine reporter mice, we reveal the choreography of early murine splenic iNKT cell activation across diverse settings of glycolipid immunization and systemic infection with *Streptococcus pneumoniae*. We find that iNKT cells consolidate in the marginal zone and require dendritic cells lining the splenic marginal zone for activation following administration of cognate glycolipids and during systemic infection but not following exogenous cytokine administration. While further establishing the importance of cognate iNKT cell interactions with antigen-presenting cells, we also show that non-cognate iNKT-dependent mechanisms are sufficient to mediate effector outcomes such as STAT signaling and DC licensing throughout the entire splenic parenchyma. Collectively, these data provide new insight into how iNKT cells may serve as a natural adjuvant in facilitating adaptive immune responses irrespective of their tissue localization.

## INTRODUCTION

Invariant natural killer T (iNKT) cells are a distinct lineage of αβ TCR+ lymphocytes that rapidly exert effector functions such as secretion of the cytokines interleukin (IL)-4 and/or interferon (IFN)-γ following encounter with lipid antigens presented in the context of the MHCI-like molecule CD1(1) or through cytokine regulated mechanisms or both(2). In addition, iNKT cells have a low threshold of activation thus providing a functional bridge between initial innate immune defense and subsequent adaptive responses. These properties, in combination with their emerging role in diverse settings including infection, cancer and metabolic syndrome(3, 4), not only indicate that iNKT cells serve a critical role in the early events of immune activation, but also provide a motivation for exploiting this cell type clinically to act as a natural adjuvant for enhancing protective immunity and/or controlling immune homeostasis. To fully realize the function of iNKT cells, as well as their potential as

[¶]For editorial concerns, please contact: Elizabeth Leadbetter, PhD, Assistant Member, Trudeau Institute, 154 Algonquin Ave. Saranac Lake, NY 12983, eleadbetter@trudeauinstitute.org, ph: 518-891-3080, fax: 518-891-5126.
[§]Contributed equally
[†]Present address: McGill University, Montreal, QC, Canada

a therapeutic target, it is critical to identify the earliest activation events of this cell type in situ.

The spleen is the primary site of systemic immune surveillance and activation in response to blood-borne antigens. In particular, the marginal zone (MZ) of the spleen, which lies just outside of the lymphocyte-residing white pulp, contains a wide vascular bed termed the marginal sinus where the arterial blood supply terminates. This site serves as the primary access point for both particulate and cellular entry into the spleen(5). The MZ contains a number of innate leukocytes specialized for rapid detection of blood-borne antigens. For example, SIGNR-1+MARCO+ macrophages lining the marginal sinus are critical for recognition and degradation of systemic pathogens and complement the function of innate-like MZ B cells that are well-established to provide early antibody production for control of systemic pathogens(5). Notably, subsets of dendritic cells also reside in the MZ and bridging channels under steady-state conditions(6), yet their role at this site is not clear. Thus, the splenic MZ is a tightly organized network of cells working together to optimally mediate rapid immunity for host protection.

Given the accelerated effector responses of iNKT cells and their relative abundance in the spleen compared to other lymphoid organs(7), it stands to reason that these innate leukocytes may also communicate with resident MZ cell types to immediately and dramatically impact the outcome of immune responses directed towards systemic infections or other foreign antigens. Specifically, iNKT cells recognize numerous bacterial glycolipids in the context of CD1d (8, 9), including one recently identified in *Streptococcus pneumonia*(10) and are robustly activated during *S. pneumonia* infection by DC-derived IL-12 plus self-glycolipid containing CD1d (11). We and others have recently shown that iNKT cells can provide cognate help to B cells resulting in extrafollicular plasmablast formation and IgM and IgG3 production reminiscent of MZ B cell activation(12–14). MZB cell antibody production is a key component of immune defense against *S. pneumoniae*(15), so B cell help from iNKT cells during this infection might be highly relevant but remains largely unstudied. Furthermore, iNKT cells have been identified by us and others as critical for survival following infection with URF918, a serotype 3 clinical isolate of *S. pneumonia*(11, 16). Systemic *S. pneumoniae* infection, described by the WHO as a significant public health threat, is responsible for the deaths of over half a million children a year, despite the introduction of multiple vaccines in the last 10 years. *S. pneumoniae* causes pulmonary pneumonia, otitis media, meningitis, and invasive disease or septicemia. *S. pneumonia* of the serotype 3 is also one of a select group of serotypes found to be associated with increased risk of death during invasive disease in humans(17), with the rate of in-hospital death for patients systemically infected with serotype 3 reaching 50%(18). As such, it is important to dissect the role of splenic iNKT cells during this systemic infection relevant to public health.

Furthermore, iNKT cells are susceptible to activation across a spectrum of stimuli, ranging from selectively TCR-CD1d-glycolipid mediated activation to TCR-CD1d-self glycolipid stimulation in combination with cytokine exposure, to exclusively cytokine dominated activation(11). The ramifications of these different forms of activation for iNKT effector function and the localization of splenic iNKT cells following stimulation by these different activators has not been described. The focus of the current study was to compare the dynamics of and cellular requirements for iNKT cell activation in response to blood-borne cognate lipid antigens as compared to systemic cytokine or complex pathogen-mediated activation. To this end, we have combined various chemokine and cytokine reporter mice with a new method of mCD1d-specific tetramer staining of fresh spleen tissue to track the localization and activation of the endogenous iNKT cell population *in situ*. Using these techniques, we find that iNKT cells are widely distributed throughout the spleen during

steady-state conditions, but rapidly consolidate in the marginal zone (MZ) following immunization with synthetic glycolipids and during systemic *S. pneumonia* infection, where they produce cytokine in a highly compartmentalized fashion. In contrast, in vivo exposure of iNKT cells to systemic cytokine fails to organize iNKT cells along the MZ despite dramatic activation and production of IFNγ. Given this localization pattern, it is not surprising that MZ dendritic cells serve as a critical contributor to iNKT cell activation in response to both glycolipids and infection but are dispensable for activation by systemic cytokines. iNKT cell cytokine production, in turn, mediates global effects on the splenic microenvironment by inducing cytokine-specific STAT phosphorylation across the splenic parenchyma and DC mobilization to the T cell zone in a non-cognate manner. Collectively, our results demonstrate that iNKT localization and site of activation is consistent with a requirement for DCs under all conditions except exogenous addition of cytokines. Furthermore, these activation conditions share a common, global effector outcome further highlighting the function of iNKT cells as a natural adjuvant during immunity and infection.

## MATERIALS AND METHODS

### Animals

4get, 4get/KN2, STAT6-deficient, and CD1d-deficient mice on a Balb/c background and CD11c-DTR.eGFP.KN2, μMT.KN2, Great (*Ifng*$^{tm3.1Lky}$), CD1d-deficient (Mark Exley, Beth Israel Deaconess Medical Center, Boston, MA), *batf3*−/−, and CXCR6-GFP+/− mice (Jackson Laboratories, Bar Harbor, ME) on a C57BL/6 background were bred and kept under specific pathogen-free conditions at the Trudeau Institute and were used at 8–12 weeks of age. All experiments were performed under Trudeau Institute Animal Care and Use Committee-approved protocols.

### Immunizations and *S. pneumoniae* infection

Mice were immunized intravenously with 0.5 μg/mouse αGalactosylceramide (αGalCer) or 40 μg/mouse GSL-1 in PBS containing 0.1%BSA and <0.25% DMSO or PBS/BSA/DMSO alone. Alternatively, some mice intravenously received IL-12 (0.5 μg) and IL-18 (1.0 μg) or $1\times10^6$ CFU *S. pneumoniae* (strain URF918, provided by K. Kawakami, University of the Ryukyus, Nishihara, Okinawa, Japan).

### Flow cytometry

iNKT cell analysis was performed by dissociating spleens through a 0.7 micron cell strainer with the end of a 5 ml syringe plunger to generate single cell suspensions followed by red blood cell lysis. For dendritic cell analysis, spleens were injected with a solution of 0.1 mg/ml Liberase TM and 20 μg/ml DNase I (Roche) in RPMI1640 (Invitrogen) and shaken for 20 minutes at 37° C. A final concentration of 5 mM EDTA diluted in fetal calf serum was added to each sample for an additional 5 minutes at 37°C. Splenocytes were filtered through a 100 um cell strainer, red cell lysed and maintained on ice for antibody staining and flow cytometric analysis. Splenocytes were stained with antibodies against TCRβ (H57-597), CD11b (M1/70) from Biolegend and huCD2 (RPA.2-10), CD11c (HL3), MHCII (M5/114.15.2), CD8α (53–6.7), B220 (RA3-6B2) from BD Biosciences. CD1d tetramers loaded with PBS57 (an αGalCer homologue) or left unloaded were obtained from the NIH Tetramer Core Facility and incubated with splenocytes at room temperature for 20 minutes prior to surface antibody staining on ice. Glycolipid loaded CD1d-tetramer is used for all FACS and confocal analysis unless otherwise noted. Intracellular IFN-γ (XMG1.2, BD Biosciences) were detected by following instructions from the eBioscience Foxp3 staining kit. Phosphorylation of STAT6 at tyrosine 641 (J71-773.58.11) and STAT1 at tyrosine 701 (4a) were detected as described previously(19). All flow cytometric data was acquired on a FACS Canto II and analyzed with Flowjo (Treestar, Inc.)

### Generation of mixed bone marrow chimeras

Bone marrow from B cell-deficient μMT mice heterozygous for the KN2 allele was mixed with either wildtype or CD1d−/− bone marrow at a 3:1 ratio and injected into the tail veins of lethally irradiated (1000 rad split into two doses) wildtype C57BL/6 hosts to generate mice selectively lacking CD1d expression by B cells. To evaluate the role of CD1d on DCs, some irradiated mice received a 50:50 mix of CD1d+/+ and CD1d−/− bone marrow. All chimeras were used for experiments 6–8 weeks following donor cell transplantation. Specific deletion of CD1d on splenic B220+ cells or CD11c+MHCII+ DCs from test chimeras was confirmed by flow cytometry.

### Diphtheria toxin and liposome administration

Mice were intraperitoneally injected with 100 ng/mouse of Diphtheria Toxin from *Corynebacterium diphtheriae* (Sigma-Aldrich, D0564) 24 hours prior to immunization with αGalCer. For liposome experiments, mice were intravenously injected with 0.2 ml of clodronate-loaded or PBS liposomes either 24 hours or 3 weeks prior to immunization with αGalCer. $Cl_2$MDP (or clodronate) was a gift of Roche Diagnostics GmbH (Mannheim, Germany) and encapsulated in liposomes as previously described(20).

### Confocal/fluorescent microscopy

For detection of GFP, YFP, and PBS57-CD1d tetramer staining, spleens were harvested and immediately placed in 5% agarose blocks for sectioning. Spleen tissue was cut into 200 micron thick sections using a vibrating microtome. Tissue antibody staining was performed on ice for 60 minutes with the exception of PBS57-CD1d or unloaded tetramer staining which was performed at room temperature for 30 minutes prior to staining with other antibodies on ice and analysis by confocal microscopy (Leica TCS SP5). Glycolipid loaded CD1d-tetramer is used for all FACS and confocal analysis unless otherwise noted. Surface antibody staining included B220, CD11c, huCD2, CD169 (3D6.112, AbD Serotec) and SIGN-R1 (22D1, eBioscience). For in situ evaluation of splenic macrophage and dendritic cells subsets, spleens were immediately frozen in optimal cutting temperature embedding compound over liquid nitrogen. Frozen spleens were cut into 6 μm sections on a cryostat (Leica) and fixed in a mixture of ice-cold 75% acetone/25% ethanol for 5 min. Sections were blocked in PBS plus 2% BSA and 5% normal mouse serum for 60 minutes prior to specific antibody staining. To quantitate localization, pixel intensity and square area was determined by Image J software for three defined regions: T cell zone (TZ), B cell follicles/zone (BZ), and Marginal Zone (MZ). Regions were defined based on labeling with CD4/8 (TZ), B220 (BZ), and SignR1 (MZ). Unit density was determined to be the ratio of specified pixel intensity per area. Normalized unit density is an expression of unit density standardized to the T zone value, that is, a ratio of specific regional unit density to T cell zone unit density.

### IL-12 ELISA

For detection of serum IL-12, ELISA plates were coated with anti-mouse IL-12p40/p70 (C15.6, BD) then blocked with 1% BSA/PBS. Serum samples were diluted in 0.1%BSA/PBS. Purified murine IL-12p40 (BD) was used for a standard curve. Bound IL-12 was detected with rat anti-mouse IL-12p40/p70-biotin (C17.8, BD) followed by streptavidin-alkaline phosphatase (BD) using pNpp (Sigma) diluted to 1mg/ml in alkaline buffer (Sigma). Plates were read on a Molecular Devices SpectramaxPlus384 ELISA reader at 405nm.

### Statistical analysis

Non-parametric t-tests and one way ANOVA tests were performed by GraphPad PRISM 5 software.

## RESULTS

### Splenic iNKT cell localization differs according to the stimulus

To determine the location of the endogenous iNKT cell population in wildtype mice under steady-state and various activating conditions, we developed an in situ technique whereby we detect glycolipid-loaded CD1d tetramer labeling of iNKT cells in fresh splenic tissue by confocal microscope (Fig. 1*A*–*N*). Antibodies against B220, CD4 and SIGN-R1 (a marker of MZ macrophages) were used to delineate the B cell follicles, T cell area and MZ, respectively. Consistent with a recent study which used confocal imaging in combination with indirect labeling techniques or transfer of purified iNKT cells into congenic recipients to follow splenic iNKT cell migration(21), we consistently found CD1d tetramer+ cells dispersed throughout the splenic white and red pulp during their endogenous resting state (Fig. 1*A,B* and data not shown). Tetramer labeling of spleens from naive NKT-deficient CD1d−/− mice demonstrated negligible background binding (Fig. 1C,*D*), as did labeling with unloaded CD1d tetramer on WT spleen sections from uninjected mice (Suppl. Fig. 1*A,B*). Kinetic experiments using upregulation of the high-affinity alpha chain of IL-2 receptor subunit (CD25) as an early marker of activation demonstrated that iNKT cells were activated within 4 hours after intravenous immunization with αGalCer (Fig. 1*E*). Similar activation kinetics were observed using intracellular IFNγ production as an outcome measure (Fig. 1*F,G*). We next determined the location of CD1d-tetramer+ iNKT cells at this time of peak activation. Four hours after αGalCer immunization, there was no significant change in the number of splenic CD1d-tetramer+ iNKT cells (Fig. 1*H*). However, confocal images and fluorescent quantification reveal that αGalCer stimulates iNKT cells to accumulate at the MZ and bridging channels of the spleen (Fig. 1*I*) as compared to vehicle injected controls (Fig. 1*K*). This is consistent with redistribution but not enhanced recruitment of this cell type from the peripheral circulation. To determine whether the iNKT cell response we observed with a synthetic lipid agonist is similar to encounter with bacterial glycolipids, Balb/c mice were immunized with a glycosphingolipid (GSL-1) expressed by the *Sphingomonadaceae* family of bacteria(9). Intravenous administration of GSL-1 resulted in rapid accumulation of iNKT cells within the MZ and bridging channels of the spleen at the same 4 hour time point as for αGalCer administration, as compared to vehicle injected controls (Fig. 1*J,K*). The observations of iNKT cell location under steady-state and glycolipid-mediated activation conditions were confirmed using heterozygous CXCR6-eGFP knock-in mice in which iNKT cells highly express eGFP (Suppl. Fig. 1*C,D*)(22). Collectively, these results indicate that iNKT cells rapidly localize to the vascular-rich region of the spleen and cluster at the MZ and bridging channels following immunization with diverse cognate lipid antigens.

In addition to cognate lipid immunization, two other forms of activation for iNKT cells have been characterized: one driven exclusively by high levels of cytokines such as IL-12 and IL-18(23) and the other induced by a combination of self-ligand-CD1d recognition plus IL-12 costimulation(2). Indeed, we have recently shown that the cytokine-driven “indirect” form of iNKT cell activation dominates the immune response during infection, even if the pathogens contain known CD1d cognate ligands(11). To compare these two other methods of iNKT cell activation to encounter of cognate antigen-mediated activation, WT mice were intravenously administered recombinant IL-12 and IL-18 or infected with *S. pneumoniae.* We determined that IFNγ production by iNKT cells peaked at 2 hours after cytokine administration and 8 hours after *S. pneumoniae* infection (Suppl. Fig. 2*A,B*). As previously

shown, IL-4 production was not detectable under either condition (data not shown)(11). Interestingly, iNKT cells also accumulated in the splenic marginal zone during infection (Fig. 1*L*). This localization pattern is the same that we detected after cognate glycolipid immunization, and suggests that the requirement for CD1d engagement dictates the localization of iNKT cells in the spleen. In contrast, intravenous IL-12 and IL-18 administration robustly activates iNKT cells, but they remain widely distributed throughout the spleen (Fig. 1*M*), reflecting the same distribution observed in PBS vehicle injected mice (Fig. 1*N*).

## Consolidation of iNKT cells yields compartmentalization of effector cytokine production

As demonstrated in our in situ tetramer labeling studies, some iNKT cells remained in the T cell zone following lipid administration. To delineate the exact location of iNKT cell activation and effector cytokine production, we used IL-4 dual reporter (4get/KN2)(24) and IFNγ reporter (Great)(25) mice. iNKT cells from 4get/KN2 mice are constitutively GFP+ due to persistent expression of IL-4 mRNA(26) and, upon activation, rapidly express huCD2 on their cell surface indicating IL-4 protein production(24, 27). Following intravenous αGalCer administration, splenic CD1d-tetramer+ iNKT cells began to express huCD2 at 2 hours with peak production occurring at 4 hours post-immunization (Fig. 2*A,B*), a kinetic similar to IFNγ production (Fig. 1*E–G*). Importantly, Figure 2A confirms that production of IL-4 (i.e. huCD2 expression) was limited to CD1d-tetramer+ iNKT cells following in vivo administration of αGalCer. This observation allowed the use of huCD2 as a marker for localizing the endogenous IL-4 producing iNKT cell population in the spleen of mice in situ. At 4 hours post-immunization of 4get/KN2 mice, we found IL-4 producing huCD2+ cells almost exclusively within the MZ and bridging channels of the spleen (Fig. 2*C left panel, D*). Mice homozygous for the 4get allele were used as a huCD2 negative staining control (Fig. 2*C middle panel*). To corroborate our flow cytometry data and confirm that huCD2 producing cells detected within the MZ were iNKT cells, we combined our in situ tetramer labeling technique with huCD2 detection. Consistent with the results described above, tetramer+ iNKT cells that co-stained with huCD2 were found outside of the white pulp clustered around the bridging channels and MZ (Fig. 2*C right panel*). To be sure that our characterization of effector cytokine secreting iNKT cells as consolidating in the MZ is not unique to IL-4-secreting iNKT cells, we evaluated localization of iNKT cells producing IFNγ using mice engineered to report IFNγ production via YFP expression (Great)(25). αGalCer immunization showed that at the time of iNKT consolidation in the MZ, the IFNγ producing cells were also consolidated in the MZ (Suppl. Fig. 2*C*) as compared to the DMSO vehicle controls (Suppl. Fig. 2*D*). At this timepoint following αGalCer, IFNγ production is largely limited to iNKT cells (data not shown), so this result is consistent with MZ consolidation of IFNγ-secreting iNKT cells. We next determined that intravenous administration of GSL-1 resulted in rapid production of IL-4 and huCD2 expression by iNKT cells with a kinetic similar to αGalCer immunization (Fig. 2*E*). Similar to our experiments using αGalCer, IL-4 producing huCD2+ iNKT cells accumulated within the MZ and bridging channels after GSL-1 administration (Fig. 2*F,G*). In summary, these results indicate that iNKT cells rapidly localize to the vascular-rich region of the spleen and produce the canonical cytokines IL-4 and IFNγ in a highly compartmentalized fashion following immunization with cognate glycolipid antigens.

These data clearly inform us as to the localization of specific IL-4 and IFNγ producing iNKT cells in response to cognate antigen. However, following recombinant cytokine administration or during *S. pneumoniae* infection the production of IFNγ by other cells, including NK1.1+TCRβ-NK cells, precludes the ability to detect iNKT-specific IFNγ production in situ during those stimulating conditions (unpublished observations). Instead, under those conditions, the localization pattern of iNKT cells as determined by confocal

imaging (Fig. 1*L,M*) at the times of peak IFNγ production by iNKT cells (Suppl. Fig. 2*A,B*) gives the clearest suggestion of localization of cytokine secreting iNKT cells.

## Marginal Zone DCs are critical for iNKT cell activation under diverse inflammatory conditions

The distinct localization patterns of iNKT cells following cognate and, to a lesser extent, pathogen activation vs. cytokine-driven stimulation prompted us to investigate which splenic antigen-presenting cell(s) are required for elaboration of the iNKT cell effector program under these conditions. Given that iNKT cells accumulate and produce IL-4 and IFNγ at the splenic marginal zone in response to cognate lipid antigen administration, we first determined the cell type resident in the MZ niche responsible for cognate activation of iNKT cells following systemic glycolipid administration, an event dependent on CD1d-restricted antigen presentation(3). Although the splenic MZ contains distinct subsets of macrophages and dendritic cells, MZ B cells express particularly high levels of CD1d(28) and are potent activators of iNKT cells in vitro (14, 29). However, analysis of mixed bone marrow chimeras in which B cells were selectively deficient in CD1d did not result in any loss of iNKT cell IL-4 production following αGalCer administration in vivo (Fig. 3*A*). A study by Schmieg et al. reported that dendritic cells were indispensable in early iNKT activation in vivo by depleting CD11c+ cells from mice expressing the simian diphtheria toxin receptor under control of the CD11c promoter (CD11c-DTR mice) prior to αGalCer administration(30). Crossing the CD11c-DTR mice to the KN2 IL-4 reporter strain, we obtained similar results using IL-4 (huCD2 expression) as an outcome measure (Fig. 3*B*). However, a recent report indicated that diphtheria toxin treatment to these mice not only depletes dendritic cells, but also CD169+ and SIGNR-1+ macrophage subsets lining the MZ(31). To investigate the potential contribution of macrophages in this system, we next depleted both macrophage subsets by intravenous administration of liposome encapsulated clodronate (CL) to wildtype mice, a well-established method of splenic macrophage depletion (Fig. 3*C*)(32). In contrast to previous observations(30), however, CL treatment also abrogated splenic iNKT cell production of IL-4 (Fig. 3*D*) despite no impact on the frequency of total splenic iNKT cells (Fig. 3*E*). Thus, further investigation into the relevant antigen-presenting cell(s) for iNKT cell activation was required.

In the course of our studies, we consistently observed a ~50% reduction in total splenic CD11c+MHCII+ dendritic cells 24 hours after CL treatment (Fig. 3*F*) with a more profound loss in the CD8+ subset than CD8− subset (Fig. 3*G*). When we examined the spleens of CL-treated mice histologically, we found selective depletion of CD11c+ cells lining the MZ, whereas the CD11c+ cells in the T cell zone appeared relatively unaffected (Fig. 3*H*), a result consistent with previous reports (33). To more closely test a role for MZ DCs vs. macrophages in early iNKT cell activation, we took advantage of the distinct reconstitution kinetics of splenic macrophages compared to dendritic cells (32). Consistent with previous observations, both SIGN-R1+ MZ and CD169+ metallophilic splenic macrophage populations remained depleted for at least 3 weeks after a single injection of CL whereas DC numbers were restored in frequency and location within one week (Fig. 4*A–C*)(31, 32). Using this strategy, we immunized mice with αGalCer at either 24 hours or 3 weeks post-CL treatment to assess iNKT cell canonical cytokine production. iNKT cell IL-4 (Fig. 4*D,E*) and IFN-γ (Fig. 4*F*) production were lost in αGalCer-immunized animals 24 hours after CL injection, a time point at which both MZ DCs and macrophages were depleted (Fig. 4*A,B*). By contrast, iNKT cell production of IL-4 in response to αGalCer immunization was completely restored in mice 3 weeks after CL treatment when macrophages were still absent, but MZ DCs had been restored. The numbers of IFNγ producing iNKT cells generated in response to αGalCer was also restored (Fig. 4*F*), but not quite to the extent achieved in intact mice, which suggests that the DCs may not be completely reconstituted

yet, or there could be different cellular requirements for iNKT production of IFNγ than for IL-4. Collectively, these results indicate MZ DCs are a critical APC for iNKT cell activation following cognate lipid immunization.

To further investigate the antigen presenting cell requirements for iNKT cell activation during systemic infection, we repeated these clodronate depletion studies with *S. pneumonia* infected mice. As expected, iNKT cells failed to become activated during *S. pneumoniae* infection in mice treated with CL 24 hours prior to infection (Fig. 5*A*). Given our previous work describing the importance of both CD1d and IL-12 from APCs to mediate iNKT activation during infection(2), these data suggested that acute treatment of mice with CL prior to pneumococcal infection eliminated either self-lipid presenting CD1d or the source of IL-12 critical for iNKT cell activation, or both. Indeed, the increase in serum IL-12p40 detected 8 hours after systemic *S. pneumoniae* infection was not observed in infected, CL-treated animals (Fig. 5*B*). Importantly, both iNKT cell activation and serum IL-12p40 levels were completely restored in mice infected 3 weeks after CL treatment (Fig. 5*A,B*), a time point in which MZ DCs, but not SIGN-R1+ macrophages were allowed to repopulate the splenic MZ. To corroborate our depletion studies and confirm the importance of DC-derived IL-12 in combination with CD1d to mediate iNKT cell activation in vivo during infection, we assessed iNKT cell activation following pneumococcal infection of *batf3*−/− mice which have a specific deletion of splenic CD8+ DCs(34). Importantly, this subset has been shown to reside in the marginal zone during homeostasis(6) and to be the dominant source of IL-12 in a number of adjuvant and infection-based models of immunity(35–37). Indeed, iNKT cells from *batf3*−/− mice produced significantly less IFNγ in response to *S. pneumoniae* infection than wildtype controls (Fig. 5*C*) which correlated with reduced serum levels of IL-12p40 from the same animals (Fig. 5*D*). The residual IFNγ production in *S. pneumoniae* infected *batf3*−/− mice could be a result of activation through cytokines and/or CD1d on other DC subsets or partial contribution of an entirely different APC(2).

One concern with the above studies was that acute treatment of CL may have off-target effects on iNKT cells and inhibit their activation irrespective of phagocyte depletion. To address this concern, we again treated animals with CL and, 24 hours later, administered recombinant IL-12 and IL-18 as described above. As shown in Figure 5E, cytokine-driven iNKT activation was similar in both PBS or CL treated immunized mice, indicating iNKT cells are not intrinsically defective under these conditions. These results also confirmed that cytokines are sufficient to activate iNKT cells, and MZ DCs are no longer required if the cytokine is extrinsically provided. Collectively, these results indicate that marginal zone-resident DCs are the critical APC responsible for presenting foreign or self-antigens and providing cytokines for iNKT cell activation during both immunization and infection.

### iNKT cells exert their effector program beyond their cognate partners

Given the restricted localization of iNKT cells under cognate activating conditions, we next considered whether iNKT cells direct their effector functions to their local site of activation. In the course of our studies, we observed that CD11c+MHCII+ DCs dramatically upregulated CCR7 expression (Fig. 6*A*) and relocated from the MZ and bridging channels to the T cell zone following αGalCer administration (Fig. 6*B*), a response previously observed following activation with TLR agonists(38, 39) or CD40-CD40L interactions(39). Importantly, DC relocation occurred in a CD1d-dependent manner (Fig. 6*B*). To consider whether this effector outcome required cognate interactions, we generated mixed bone marrow chimeras in which 50% of DCs lacked CD1d expression but 50% of DCs expressed normal levels of CD1d (Fig. 6*C,D*). Unexpectedly, we found that cognate iNKT-DC interactions were dispensable for upregulation of CCR7 by splenic DCs as both CD1d+ and CD1d− DCs in these chimeras equally upregulated CCR7 expression after αGalCer immunization (Fig. 6*E*). We have also previously demonstrated that during infection, despite

localized production, cytokine signaling can saturate the entire immune compartment of lymphoid organs(19). Given that iNKT cell activation can take place, depending on the stimulus, at distinct loci within the splenic parenchyma, we further postulated that the effector range of their cytokines extend beyond their immediate microenvironment. To interrogate this question, we measured the levels of phospho-STAT6 and phospho-STAT1 in the total splenic B cell compartment as readouts of IL-4 and IFNγ signaling, respectively, by intracellular flow cytometry(19). Although we found iNKT-derived IL-4 and IFNγ to be produced in a tightly restricted manner in proximity to the MZ of the spleen (Fig. 1,2), FACS analysis detected high levels of both phospho-STAT6 and phospho-STAT1 in the entire splenic B220+ B cell population within 4hrs after αGalCer administration in a CD1d-dependent manner (Fig. 6*F–H*). Because all splenic B cells show evidence of having received IL-4 signals, these results suggest that irrespective of the location in which iNKT cells are activated they contain the potential to condition the entire lymphoid organ environment to either regulate or potentiate the immune response.

## DISCUSSION

The inability to localize and track the endogenous iNKT population as they initiate their effector program in vivo has been a long-standing roadblock to advancing our understanding of this innate T lymphocyte subset. Other groups have tried unsuccessfully to identify endogenous individual splenic NKT cells by tetramer in WT mice(40, 41) and instead have utilized TCRβ NK1.1 labeling of endogenous cells, adoptive transfer of sorted iNKT cells or fluorescent diffusion strategies(21) to probe the localization of iNKT cells in a post-transfer state. These approaches have found the majority of resting iNKT cells to be localized in the PALS(41) or in the MZ, PALS, and red pulp(21). However, using a novel method of *in situ* mCD1d tetramer staining, in combination with relevant cytokine reporter mice, we can now unambiguously identify a restricted localization and cytokine production profile for endogenous splenic iNKT cells. In agreement with previously published reports, we find that endogenous iNKT cells are widely and evenly distributed throughout the parenchyma of the spleen, including B and T cell follicles in the PALS, the MZ, and red pulp (data not shown). Importantly, we find that this distribution only changes to a restricted MZ localization following cognate activation by model and bacterially-derived glycolipids or *S. pneumonia* infection, presumably as a result of arrest in proximity to antigen loaded APCs. Batista, Barral, and colleagues have previously shown that iNKT cells arrest near lymph node subcapsular sinus macrophages in response to particulate glycolipid antigen(42), and similarly describe how iNKT cells arrest in the marginal zone in close proximity to antigen-rich regions within 2 hours of administration of particulate αGalCer(21). This is consistent with live imaging studies from the Kubes lab characterizing iNKT arrest in the liver following Kupffer cell capture and presentation of *Borrelia burgdorferi* antigens(43). Michael Dustin and colleagues provided the earliest description of iNKT cell arrest in the liver in response to αGalCer and GSL-1(22, 44). Interestingly, the Dustin group also found that iNKT cells arrest in the liver in response to systemic IL-12 plus IL-18(44). This contrasts with our data showing that iNKT cells remain widely and evenly distributed throughout the spleen following activation by systemic cytokines. The difference between our findings and those of the Dustin group could be explained by the different subsets of iNKT cells or antigen presenting cells which populate the spleen vs. liver or could be a consequence of different integrin or chemokine trafficking requirements, or both. The MZ is often invoked as the likely point of interaction for iNKT cells and activating APCs bearing pathogens and pathogen-derived antigens collected from the blood flowing into the spleen through the marginal sinus(14). Our data showing consolidation by activated iNKT cells and the requirement for MZDCs after glycolipid immunization and during systemic infection is also consistent with a key activation mechanism of iNKT cells being via engagement of CD1d-presented foreign or self-antigen in the MZ(11).

iNKT cells can be activated by a combination of TCR-mediated recognition of CD1d and TCR-independent activation by cytokines on a sliding scale of relative ratios(45). Specifically, iNKT cells are activated to produce IFNγ and IL-4 by TCR recognition of the glycolipids tested here in the context of CD1d. They can also produce IFNγ following TCR engagement of CD1d presenting self-glycolipids when receiving costimulation from IL-12. Finally, a robust cocktail of systemic IL-12 plus IL-18 in the absence of CD1d can also drive iNKT cells to produce copious IFNγ(45). Despite these diverse activation approaches, we found MZ dendritic cells to be a critical bottleneck for most forms of iNKT cell activation in vivo. In the case of glycolipid administration, MZDCs are likely capturing and presenting cognate glycolipid antigen directly(21), thus requiring redistribution of splenic iNKT cells. During infection, recognition of *S. pneumoniae* by MZDCs via pattern recognition receptors stimulates production and release of soluble IL-12 which combines with self-glycolipid presentation by CD1d to activate iNKT cells(2, 11). At the other end of the spectrum, iNKT cells can be activated-in-place throughout the parenchyma of the spleen by systemic administration of IL-12 plus IL-18. MZDCs are also a very likely source of systemic IL-12 and IL-18 that would be generated by physiologic conditions, but we have eliminated this step for MZDCs in our system when we provide the cytokines ex vivo. In summary, MZDCs are critical partners for iNKT cells in the spleen during their response to a myriad of different forms of activating stimuli from cognate glycolipids to systemic infection.

Much of the literature describing iNKT cell responses to antigen, interaction with other cells, and receiving of helper signals from DCs, MZB cells, B helper neutrophils, macrophages, eosinophils, and basophils, considers iNKT localization to be oriented around the marginal zone during activation(46, 47). Successful use of our new in situ iNKT cell labeling technique employing lineage-specific tetramers suggests that the conditions which produce MZ localization of iNKT cells are relevant for iNKT responses to both highly pure glycolipid antigens and systemic infections. Furthermore, early production of IFNγ by this population of iNKT cells throughout the spleen conditions the entire environment for a rapid coordinated immune defense, including enhancing activation of innate responders like NK cells, macrophages, dendritic cells, and neutrophils as well as driving relevant activation of adaptive defenders such as CD4 T cells and B cells. Perhaps as one example of this, we also noted iNKT-dependent upregulation of CCR7 and relocation by MZDCs from the marginal zone and bridging channels into the T cell zone in the spleens of mice immunized with αGalCer. Furthermore, we demonstrate that these changes, evidence of DC licensing, occur independent of cognate interactions with iNKT cells. That is, the DCs themselves do not need to specifically engage an iNKT cell via CD1d to receive this licensing signal, suggesting iNKT cells mediate this aspect of DC licensing via a soluble mediator. The specific soluble factor(s) mediating DC relocation to the T cell zone requires further investigation.

In summary, our data suggests that iNKT cells employ diverse methods to exert their effector functions, the results of which can have a profound effect on the entire lymphoid tissue landscape, further exemplifying their critical role as a bridge between innate and adaptive immune responses. In the future, combining tetramer labeling of fresh tissue sections for confocal imaging with genetically engineered reporter or gene deficient mice will provide a unique approach to dissecting the migration requirements for splenic iNKT cells under various conditions and to answer many future questions about the kinetics and localization of iNKT cells in other primary and secondary lymphoid organs.

## Supplementary Material

Refer to Web version on PubMed Central for supplementary material.

## Acknowledgments

This work was supported by the Trudeau Institute and the National Institutes of Health (R01 AI0764).

## References

1. Cohen NR, Garg S, Brenner MB. Antigen Presentation by CD1 Lipids, T Cells, and NKT Cells in Microbial Immunity. Adv Immunol. 2009; 102:1–94. [PubMed: 19477319]
2. Brigl M, Bry L, Kent SC, Gumperz JE, Brenner MB. Mechanism of CD1d-restricted natural killer T cell activation during microbial infection. Nat Immunol. 2003; 4:1230–1237. [PubMed: 14578883]
3. Van Kaer L V, Parekh V, Wu L. Invariant natural killer T cells: bridging innate and adaptive immunity. Cell and tissue research. 2011; 343:43–55. [PubMed: 20734065]
4. Tupin E, Kinjo Y, Kronenberg M. The unique role of natural killer T cells in the response to microorganisms. Nature reviews Microbiology. 2007; 5:405–417.
5. Mebius RE, Kraal G. Structure and function of the spleen. Nature reviews Immunology. 2005; 5:606–616.
6. Idoyaga J, Suda N, Suda K, Park CG, Steinman RM. Antibody to Langerin/CD207 localizes large numbers of CD8alpha+ dendritic cells to the marginal zone of mouse spleen. Proceedings of the National Academy of Sciences of the United States of America. 2009; 106:1524–1529. [PubMed: 19168629]
7. Benlagha K, Bendelac A. CD1d-restricted mouse V alpha 14 and human V alpha 24 T cells: lymphocytes of innate immunity. Semin Immunol. 2000; 12:537–542. [PubMed: 11145859]
8. Kinjo Y, Wu D, Kim G, Xing GW, Poles MA, Ho DD, Tsuji M, Kawahara K, Wong CH, Kronenberg M. Recognition of bacterial glycosphingolipids by natural killer T cells. Nature. 2005; 434:520–525. [PubMed: 15791257]
9. Kinjo Y, Tupin E, Wu D, Fujio M, Garcia-Navarro R, Benhnia MR, Zajonc DM, Ben-Menachem G, Ainge GD, Painter GF, Khurana A, Hoebe K, Behar SM, Beutler B, Wilson IA, Tsuji M, Sellati TJ, Wong CH, Kronenberg M. Natural killer T cells recognize diacylglycerol antigens from pathogenic bacteria. Nature immunology. 2006; 7:978–986. [PubMed: 16921381]
10. Kinjo Y, Illarionov P, Vela JL, Pei B, Girardi E, Li X, Li Y, Imamura M, Kaneko Y, Okawara A, Miyazaki Y, Gomez-Velasco A, Rogers P, Dahesh S, Uchiyama S, Khurana A, Kawahara K, Yesilkaya H, Andrew PW, Wong CH, Kawakami K, Nizet V, Besra GS, Tsuji M, Zajonc DM, Kronenberg M. Invariant natural killer T cells recognize glycolipids from pathogenic Gram-positive bacteria. Nature immunology. 2011; 12:966–974. [PubMed: 21892173]
11. Brigl M, Tatituri RV, Watts GF, Bhowruth V, Leadbetter EA, Barton N, Cohen NR, Hsu FF, Besra GS, Brenner MB. Innate and cytokine-driven signals, rather than microbial antigens, dominate in natural killer T cell activation during microbial infection. The Journal of experimental medicine. 2011; 208:1163–1177. [PubMed: 21555485]
12. King IL, Fortier A, Tighe M, Dibble J, Watts GF, Veerapen N, Haberman AM, Besra GS, Mohrs M, Brenner MB, Leadbetter EA. Invariant natural killer T cells direct B cell responses to cognate lipid antigen in an IL-21-dependent manner. Nature immunology. 2012; 13:44–50. [PubMed: 22120118]
13. Chang PP, Barral P, Fitch J, Pratama A, Ma CS, Kallies A, Hogan JJ, Cerundolo V, Tangye SG, Bittman R, Nutt SL, Brink R, Godfrey DI, Batista FD, Vinuesa CG. Identification of Bcl-6-dependent follicular helper NKT cells that provide cognate help for B cell responses. Nature immunology. 2012; 13:35–43. [PubMed: 22120117]
14. Leadbetter EA, Brigl M, Illarionov P, Cohen N, Luteran MC, Pillai S, Besra GS, Brenner MB. NK T cells provide lipid antigen-specific cognate help for B cells. Proc Natl Acad Sci U S A. 2008; 105:8339–8344. [PubMed: 18550809]
15. Lopes-Carvalho T, Foote J, Kearney JF. Marginal zone B cells in lymphocyte activation and regulation. Curr Opin Immunol. 2005; 17:244–250. [PubMed: 15886113]
16. Kawakami K, Yamamoto N, Kinjo Y, Miyagi K, Nakasone C, Uezu K, Kinjo T, Nakayama T, Taniguchi M, Saito A. Critical role of Valpha14+ natural killer T cells in the innate phase of host

protection against Streptococcus pneumoniae infection. Eur J Immunol. 2003; 33:3322–3330. [PubMed: 14635040]

17. Martens P, Worm SW, Lundgren B, Konradsen HB, Benfield T. Serotype-specific mortality from invasive Streptococcus pneumoniae disease revisited. BMC infectious diseases. 2004; 4:21. [PubMed: 15228629]
18. Weinberger DM, Harboe ZB, Sanders EA, Ndiritu M, Klugman KP, Ruckinger S, Dagan R, Adegbola R, Cutts F, Johnson HL, O'Brien KL, Scott JA, Lipsitch M. Association of serotype with risk of death due to pneumococcal pneumonia: a meta-analysis. Clinical infectious diseases: an official publication of the Infectious Diseases Society of America. 2010; 51:692–699. [PubMed: 20715907]
19. Perona-Wright G, Mohrs K, Mohrs M. Sustained signaling by canonical helper T cell cytokines throughout the reactive lymph node. Nature immunology. 2010; 11:520–526. [PubMed: 20418876]
20. Van Rooijen N, Sanders A. Liposome mediated depletion of macrophages: mechanism of action, preparation of liposomes and applications. Journal of immunological methods. 1994; 174:83–93. [PubMed: 8083541]
21. Barral P, Sanchez-Nino MD, van Rooijen N, Cerundolo V, Batista FD. The location of splenic NKT cells favours their rapid activation by blood-borne antigen. The EMBO journal. 2012; 31:2378–2390. [PubMed: 22505026]
22. Geissmann F, Cameron TO, Sidobre S, Manlongat N, Kronenberg M, Briskin MJ, Dustin ML, Littman DR. Intravascular immune surveillance by CXCR6+ NKT cells patrolling liver sinusoids. PLoS biology. 2005; 3:e113. [PubMed: 15799695]
23. Nagarajan NA, Kronenberg M. Invariant NKT cells amplify the innate immune response to lipopolysaccharide. Journal of immunology. 2007; 178:2706–2713.
24. Mohrs K, Wakil AE, Killeen N, Locksley RM, Mohrs M. A two-step process for cytokine production revealed by IL-4 dual-reporter mice. Immunity. 2005; 23:419–429. [PubMed: 16226507]
25. Reinhardt RL, Liang HE, Locksley RM. Cytokine-secreting follicular T cells shape the antibody repertoire. Nature immunology. 2009; 10:385–393. [PubMed: 19252490]
26. Stetson DB, Mohrs M, Reinhardt RL, Baron JL, Wang ZE, Gapin L, Kronenberg M, Locksley RM. Constitutive cytokine mRNAs mark natural killer (NK) and NK T cells poised for rapid effector function. J Exp Med. 2003; 198:1069–1076. [PubMed: 14530376]
27. Dickgreber N, Farrand KJ, van Panhuys N, Knight DA, McKee SJ, Chong ML, Miranda-Hernandez S, Baxter AG, Locksley RM, Le Gros G, Hermans IF. Immature murine NKT cells pass through a stage of developmentally programmed innate IL-4 secretion. Journal of leukocyte biology. 2012; 92:999–1009. [PubMed: 22941735]
28. Roark JH, Park SH, Jayawardena J, Kavita U, Shannon M, Bendelac A. CD1.1 expression by mouse antigen-presenting cells and marginal zone B cells. J Immunol. 1998; 160:3121–3127. [PubMed: 9531266]
29. Barral P, Eckl-Dorna J, Harwood NE, De Santo C, Salio M, Illarionov P, Besra GS, Cerundolo V, Batista FD. B cell receptor-mediated uptake of CD1d-restricted antigen augments antibody responses by recruiting invariant NKT cell help in vivo. Proc Natl Acad Sci U S A. 2008; 105:8345–8350. [PubMed: 18550831]
30. Schmieg J, Yang G, Franck RW, Van Rooijen N, Tsuji M. Glycolipid presentation to natural killer T cells differs in an organ-dependent fashion. Proceedings of the National Academy of Sciences of the United States of America. 2005; 102:1127–1132. [PubMed: 15644449]
31. Probst HC, Tschannen K, Odermatt B, Schwendener R, Zinkernagel RM, Van Den Broek M. Histological analysis of CD11c-DTR/GFP mice after in vivo depletion of dendritic cells. Clinical and experimental immunology. 2005; 141:398–404. [PubMed: 16045728]
32. Van Rooijen N, Salomon B, van Rooijen N, Klatzmann D, van Ewijk W. Heterogeneity of mouse spleen dendritic cells: in vivo phagocytic activity, expression of macrophage markers, and subpopulation turnover. Journal of immunology. 1998; 160:2166–2173.
34. Hildner K, Edelson BT, Purtha WE, Diamond M, Matsushita H, Kohyama M, Calderon B, Schraml BU, Unanue ER, Diamond MS, Schreiber RD, Murphy TL, Murphy KM. Batf3

deficiency reveals a critical role for CD8alpha+ dendritic cells in cytotoxic T cell immunity. Science. 2008; 322:1097–1100. [PubMed: 19008445]

35. Maldonado-Lopez R, De Smedt T, Pajak B, Heirman C, Thielemans K, Leo O, Urbain J, Maliszewski CR, Moser M. Role of CD8alpha+ and CD8alpha-dendritic cells in the induction of primary immune responses in vivo. Journal of leukocyte biology. 1999; 66:242–246. [PubMed: 10449161]
36. Mashayekhi M, Sandau MM, Dunay IR, Frickel EM, Khan A, Goldszmid RS, Sher A, Ploegh HL, Murphy TL, Sibley LD, Murphy KM. CD8alpha(+) dendritic cells are the critical source of interleukin-12 that controls acute infection by Toxoplasma gondii tachyzoites. Immunity. 2011; 35:249–259. [PubMed: 21867928]
37. Farrand KJ, Dickgreber N, Stoitzner P, Ronchese F, Petersen TR, Hermans IF. Langerin+ CD8alpha+ dendritic cells are critical for cross-priming and IL-12 production in response to systemic antigens. Journal of immunology. 2009; 183:7732–7742.
38. De Smedt T, Pajak B, Muraille E, Lespagnard L, Heinen E, De Baetselier P, Urbain J, Leo O, Moser M. Regulation of dendritic cell numbers and maturation by lipopolysaccharide in vivo. The Journal of experimental medicine. 1996; 184:1413–1424. [PubMed: 8879213]
39. Reis e Sousa C, Hieny S, Scharton-Kersten T, Jankovic D, Charest H, Germain RN, Sher A. In vivo microbial stimulation induces rapid CD40 ligand-independent production of interleukin 12 by dendritic cells and their redistribution to T cell areas. The Journal of experimental medicine. 1997; 186:1819–1829. [PubMed: 9382881]
40. Berzins SP, Smyth MJ, Godfrey DI. Working with NKT cells--pitfalls and practicalities. Current opinion in immunology. 2005; 17:448–454. [PubMed: 15963710]
41. Thomas SY, Scanlon ST, Griewank KG, Constantinides MG, Savage AK, Barr KA, Meng F, Luster AD, Bendelac A. PLZF induces an intravascular surveillance program mediated by long-lived LFA-1-ICAM-1 interactions. The Journal of experimental medicine. 2011; 208:1179–1188. [PubMed: 21624939]
42. Barral P, Polzella P, Bruckbauer A, van Rooijen N, Besra GS, Cerundolo V, Batista FD. CD169(+) macrophages present lipid antigens to mediate early activation of iNKT cells in lymph nodes. Nature immunology. 2010; 11:303–312. [PubMed: 20228797]
43. Lee WY, Moriarty TJ, Wong CH, Zhou H, Strieter RM, van Rooijen N, Chaconas G, Kubes P. An intravascular immune response to Borrelia burgdorferi involves Kupffer cells and iNKT cells. Nature immunology. 2010; 11:295–302. [PubMed: 20228796]
44. Velazquez P, Cameron TO, Kinjo Y, Nagarajan N, Kronenberg M, Dustin ML. Cutting edge: activation by innate cytokines or microbial antigens can cause arrest of natural killer T cell patrolling of liver sinusoids. Journal of immunology. 2008; 180:2024–2028.
45. Brigl M, Brenner MB. How invariant natural killer T cells respond to infection by recognizing microbial or endogenous lipid antigens. Seminars in immunology. 2010; 22:79–86. [PubMed: 19948416]
46. Puga I, Cols M, Barra CM, He B, Cassis L, Gentile M, Comerma L, Chorny A, Shan M, Xu W, Magri G, Knowles DM, Tam W, Chiu A, Bussel JB, Serrano S, Lorenta JA, Bellosillo B, Lloreta J, Juanpere N, Alameda F, Baro T, de Heredia CD, Toran N, Catala A, Torrebadell M, Fortuny C, Cusi V, Carreras C, Diaz GA, Blander JM, Farber CM, Silvestri G, Cunningham-Rundles C, Calvillo M, Dufour C, Notarangelo LD, Lougaris V, Plebani A, Casanova JL, Ganal SC, Diefenbach A, Arostegui JI, Juan M, Yague J, Mahlaoui N, Donadieu J, Chen K, Cerutti A. B cell-helper neutrophils stimulate the diversification and production of immunoglobulin in the marginal zone of the spleen. Nature immunology. 2012; 13:170–180. [PubMed: 22197976]
47. Bialecki E, Paget C, Fontaine J, Capron M, Trottein F, Faveeuw C. Role of marginal zone B lymphocytes in invariant NKT cell activation. Journal of immunology. 2009; 182:6105–6113.

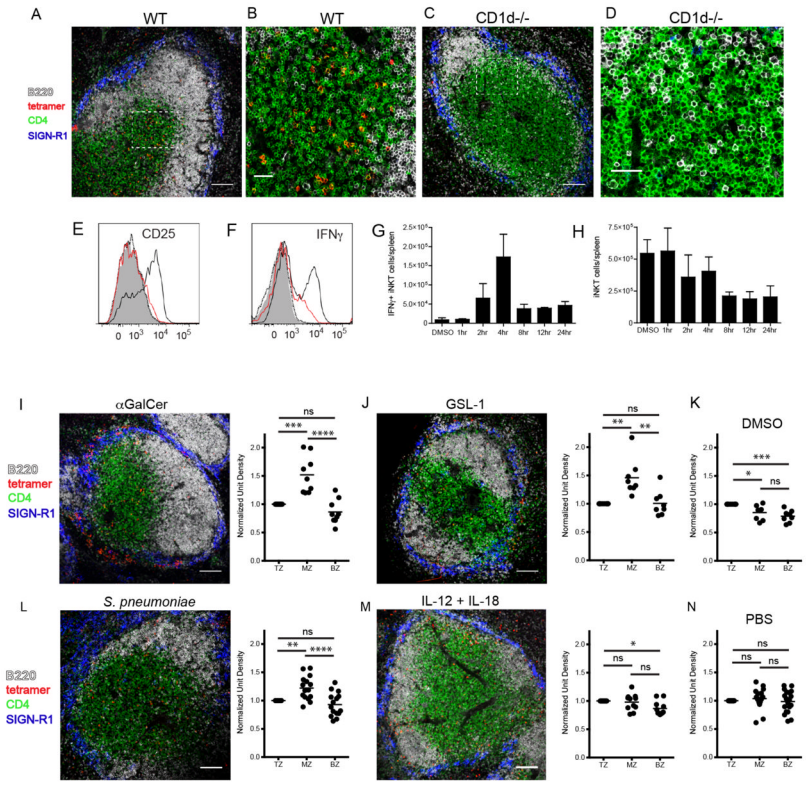


**Figure 1.**

Localization of iNKT cells under steady-state and various activating conditions. (*A–D*) Confocal images of CD1d tetramer labeling of spleen sections from unimmunized wildtype (*A,B*) or CD1d-deficient Balb/c mice (*C,D*). (*B and D*) Show the dashed insets in *A* and *C*, respectively, at higher magnification. (*E*) Histogram depicting FACS measurement of CD25 expression by CD1d-tetramer+ splenocytes at 1hr (dotted), 2hr (red) and 4hr (solid black) following immunization. The filled histogram represents the DMSO vehicle control at 4 hours post-immunization. (*F*) Histogram depicting intracellular IFNγ by tetramer+ cells as described in E. (*G*) Bar graph indicating the number of IFNγ-producing CD1d-tetramer+ splenocytes detected by FACS analysis at various time points after DMSO vehicle or αGalCer immunization. (*H*) The total number of CD1d-tetramer+ iNKT cells per spleen detected by FACS following DMSO vehicle or αGalCer immunization over time. (*I–N*) Confocal images and quantitation of CD1d tetramer labeling of spleen sections from Balb/c mice immunized 4 hours prior with αGalCer (*I*) or GSL-1 (*J*), 8 hours prior with *S. pneumoniae* (*L), or* 2 hours prior with IL-12 + IL-18 (*M*). (K) and (N) show DMSO and PBS vehicle controls. The quantification of these confocal images is performed as described in Materials and Methods. TZ, T cell zone; MZ, marginal zone; BZ, B cell zone. All data shown is representative of three experiments with two mice per group. Scale bar equals 100 μm (*A, C, I, J, L, M)* and 30 μm (*B,D*). *p<0.05, **P<0.001, ***p<0.0001, ****p<0.00001; ns, not significant.

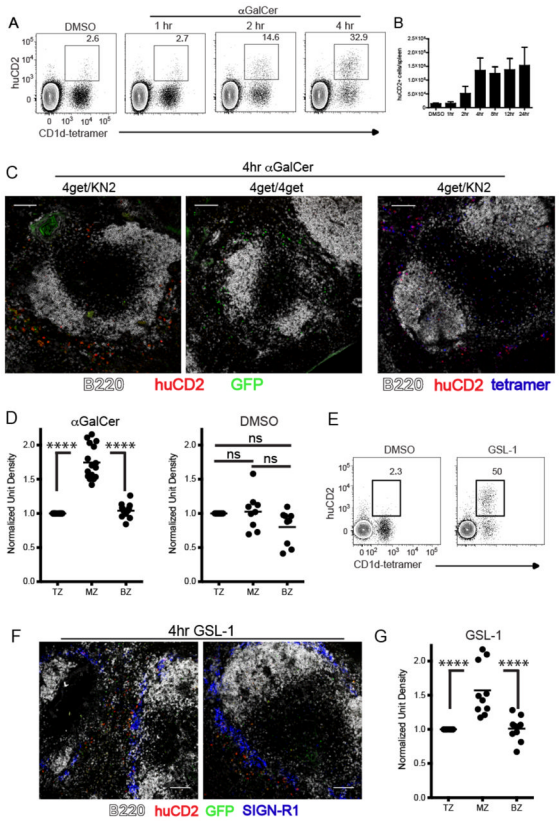


**Figure 2.**

Early IL-4 production by iNKT cells occurs at the splenic marginal zone. (*A*) 4get/KN2 mice were immunized with either DMSO vehicle or αGalCer and live B220- splenocytes were assessed for expression of huCD2 (IL-4 production) by flow cytometry at the time points indicated. Numbers represent the frequency of huCD2+ cells of the CD1d tetramer+ population. DMSO vehicle treated mice were assessed at 4 hours post-immunization. (*B*) The total number of huCD2+ cells per spleen at various time points following DMSO vehicle or αGalCer immunization. (*C*) Spleens were harvested from αGalCer-immunized 4get/KN2 or 4get/4get mice and assessed for localization of huCD2 expression as described in Materials and Methods. (*D*) Quantitation of huCD2 labeling intensity in distinct splenic regions following αGalCer or DMSO vehicle immunization as described in Figure 1. *(E)* 4get/KN2 mice were immunized with either DMSO vehicle or GSL-1 and live B220- splenocytes were assessed for huCD2 expression at 4 hours post-immunization. Numbers represent the frequency of huCD2+ cells of the CD1d tetramer+ population. (*F*) Spleens harvested from GSL-1-immunized 4get/KN2 were assessed for location of huCD2 expression. SIGN-R1 delineates the MZ. (G) Quantitation of huCD2 labeling intensity in distinct splenic regions following GSL-1 immunization. Scale bar, 100 μm. All data shown is representative of at least 3 individual experiments with 3–4 mice per group. Error bars represent standard deviation. ****p<0.00001; ns, not significant.

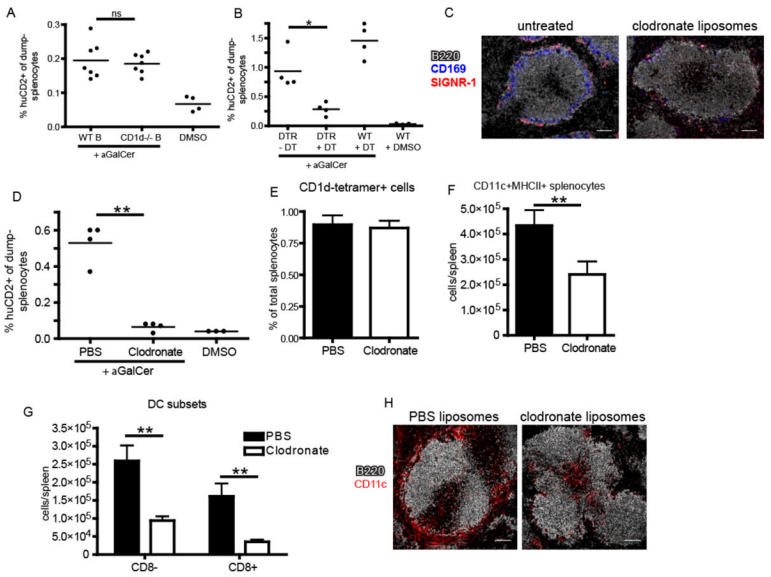


**Figure 3.**

Depletion of marginal zone phagocytes compromises iNKT cell activation. (*A*) Frequency of IL-4 producing huCD2+dump-(B220-CD11b-) splenocytes following αGalCer or DMSO vehicle immunization of bone marrow chimeras containing either WT or CD1d−/− B cells as described in Material and Methods. (*B*) Frequency of huCD2+dump- splenocytes following αGalCer or DMSO vehicle immunization of B6.KN2 (WT) or CD11c-DTR.KN2 (DTR) mice 24 hours after DT or PBS treatment. (*C*) Confocal images of spleen sections depicting the effects of CL treatment on the SIGNR-1+ marginal zone and CD169+ metallophilic macrophage subsets. (*D*) Frequency of huCD2+dump- splenocytes following αGalCer or DMSO vehicle immunization of 4get/KN2 mice treated 24 hours prior with either clodronate-loaded or PBS liposomes. (*E*) Frequency of splenic CD1d-tetramer+ cells under the conditions described in D. (*F, G*) Absolute number of total CD11c+MHCII+ dendritic cells or CD8+ and CD8− DC subsets 24 hours after PBS or CL treatment. (*H*) Spleen sections showing the localization of total CD11c+ splenocytes following PBS or CL injection 24 hours earlier. Data shown is representative of two (*A–C*) or three (*D–F*) individual experiments with three or more mice per group. Scale bar, 100 μm. Error bars represent standard deviation. * $p < 0.05$; ** $p < 0.001$; ns, not significant.

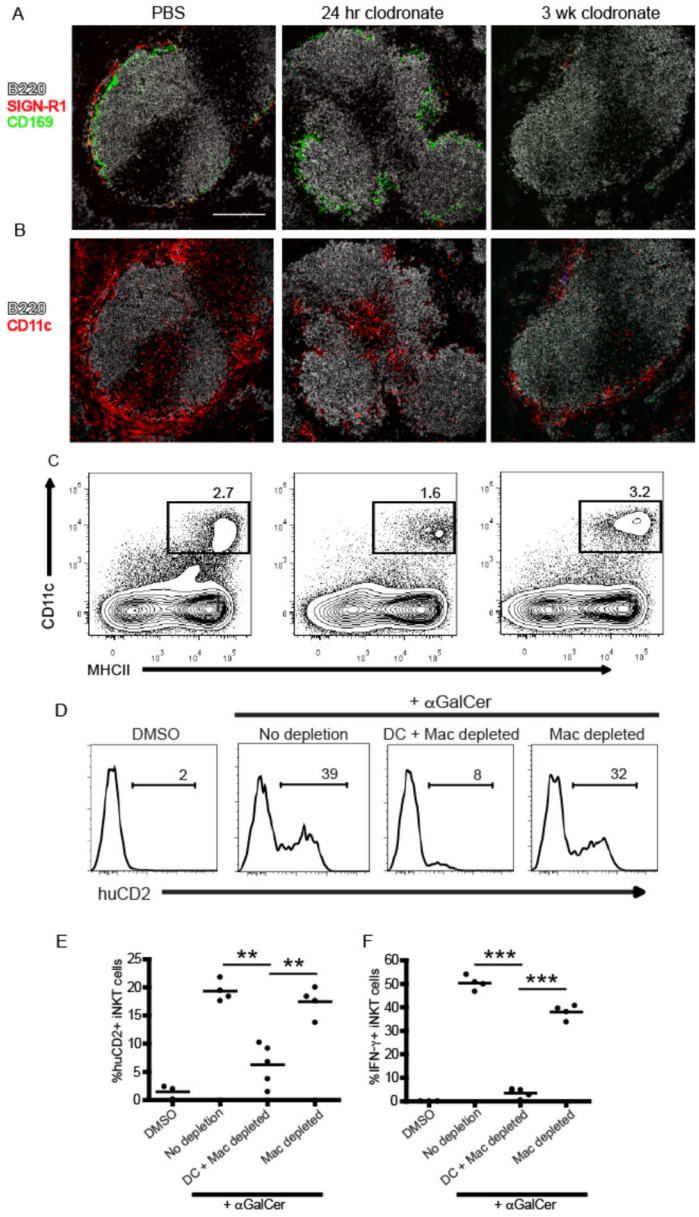


**Figure 4.**

Marginal zone DCs mediate cytokine production by iNKT cells. (*A,B*) Immunofluorescent images of spleen sections from 4get/KN2 mice 24 hours or three weeks after CL treatment. Mice treated with PBS liposomes are shown for comparison. Scale bar, 200 μm. (*C*) Contour plots showing the frequency of total splenic CD11c+MHCII+ DCs at each time point described in *A*. (*D, E*) Percentages of CD1d-tetramer+ producing IL-4 (huCD2+) splenocytes from representative individuals are shown as histograms (*D*). A summary of the percentages of IL-4 (huCD2+) (*E*) and IFNγ (*F*) producing iNKT cells after DMSO vehicle or αGalCer immunization from all 4get/KN2 mice treated with PBS or CLs is shown for conditions indicated. Results shown are representative of two individual experiments with 3–5 mice per group. ** $p < 0.001$, ***$p<0.0001$.

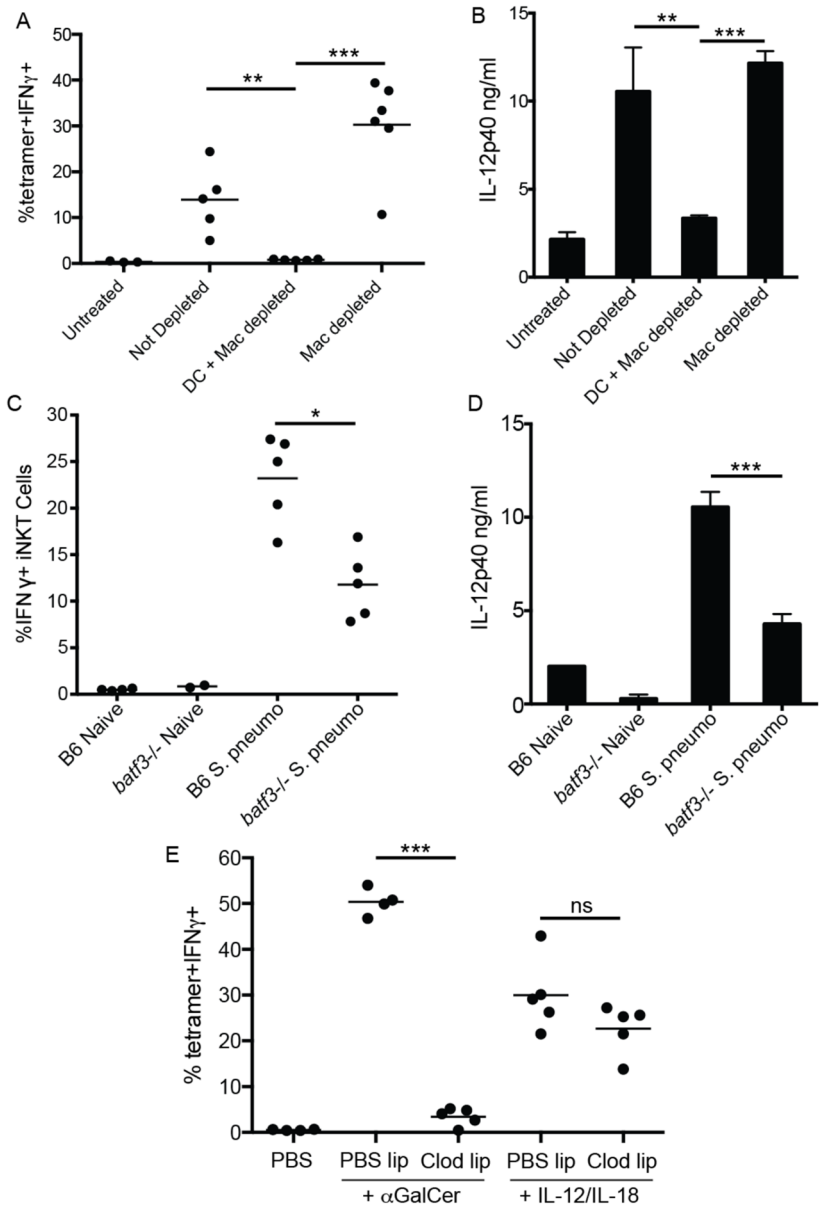


**Figure 5.**

CD8+ marginal zone DCs play a critical role in iNKT cell cytokine production following pneumococcal infection. (*A*) The frequency of IFNγ-producing iNKT cells or (*B*) serum IL-12p40 levels in *S. pneumoniae* infected animals under conditions shown in Fig. 4A. (*C*) The frequency of IFNγ-producing iNKT cells or (*D*) serum IL-12p40 levels in naïve or *S. pneumonaie* infected WT or *batf3−/−* animals. (*E*) The frequency of IFNγ producing iNKT cells following PBS, αGalCer, or IL-12/IL-18 administration 24 hours after clodronate-mediated phagocyte depletion. Data are representative of three (*E*) and two (*A–D*) experiments. Error bars represent standard deviation of at least three mice per group. * p<0.02; ** p<0.001; *** p<0.0001;ns, not significant.

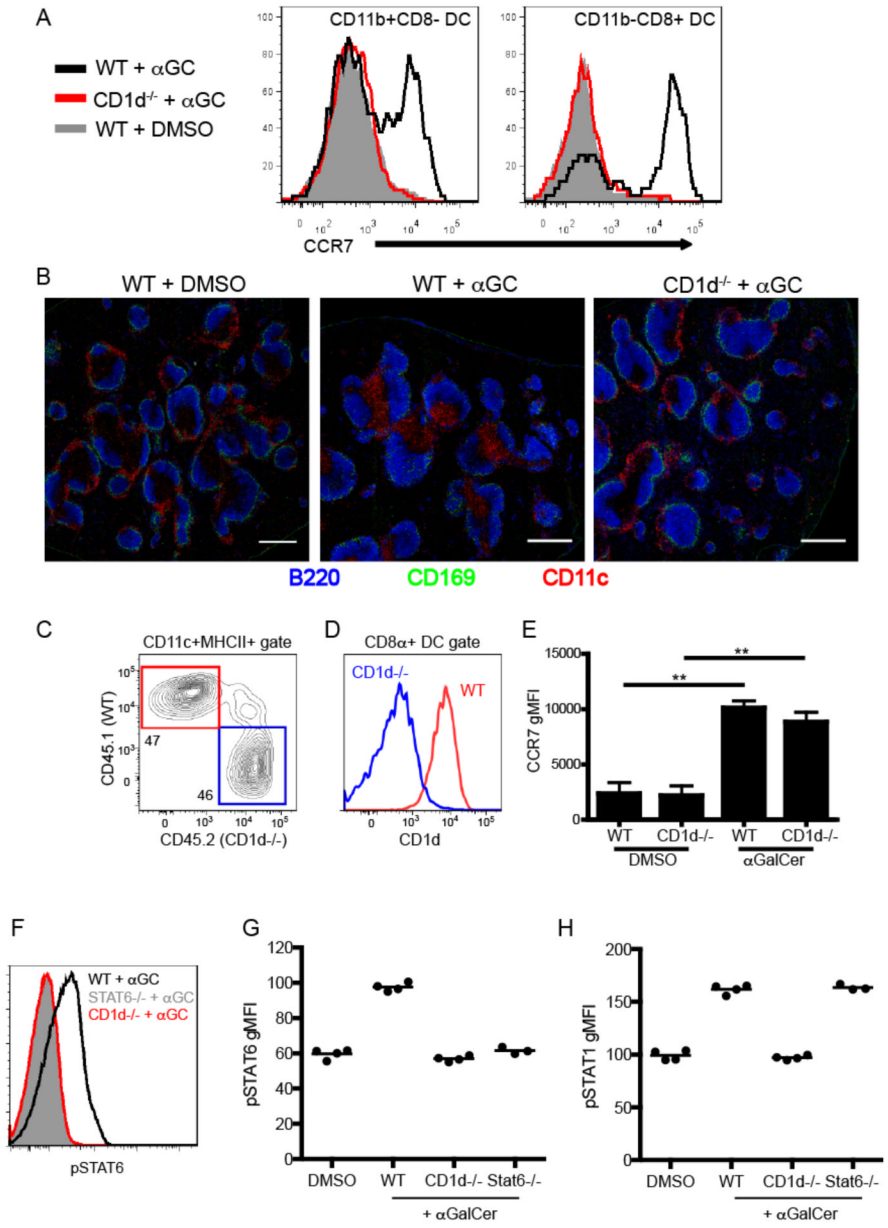


**Figure 6.**

Non-cognate effector functions of iNKT cells in vivo. (*A*) Histograms showing CCR7 expression of either CD11b+CD8− (left panel) or CD11b-CD8+ (right panel) dendritic cells from WT or CD1d-deficient mice 12 hours after immunization with αGalCer or DMSO vehicle. (*B*) Confocal microscopy analysis of spleen sections from WT or CD1d-deficient mice 12 hours after immunization with αGalCer or DMSO vehicle. Scale bar, 200 μm. (*C*) Frequency of CD45.1+ WT or CD45.2+ CD1d−/− DCs from unimmunized mixed chimeric mice as described in Materials and Methods. (*D*) CD1d expression by WT or CD1d−/− CD8α+ DCs from mixed chimeras. (*E*) Graph depicts the CCR7 geometric MFI of WT or CD1d−/− CD8α+ DCs in mixed chimera from DMSO vehicle or αGalCer immunized mice at the 12hr time point. ** p<0.001 (*F*) Phosphorylation of STAT6 in the total B220+ splenocyte population was assessed by flow cytometry in WT, CD1d−/− and STAT6−-− mice 4 hours after αGalCer immunization. (*G, H*) Geometric MFI of pSTAT6 (*G*) and

pSTAT1 (*H*) after DMSO vehicle or αGalCer immunization in indicated groups of mice. All data shown is representative of at least 2 individual experiments with 3–4 mice per group.